Enhanced CO_2 bio-utilization with a liquid-liquid membrane contactor in a bench-scale microalgae raceway pond

X. Xu [a,b], G. J. O. Martin[b], S. E. Kentish[a*]

[a] Peter Cook Centre for CCS Research, Department of Chemical Engineering, The University of Melbourne, Parkville, Victoria 3010, Australia.

[b] Algal Processing Group, Department of Chemical Engineering, The University of Melbourne, Parkville, Victoria 3010, Australia

Abstract

Microalgae are able to absorb CO_2 generated from sources such as flue gas to produce biomass with high lipid content. In this research, an immersed liquid-liquid membrane contactor was investigated to deliver CO_2 captured by a chemical solvent to the microalgae culture via semipermeable membranes. Experiments showed that the CO_2 mass transfer could be facilitated by using a thinner membrane support layer, or avoiding a support altogether, as the support was liquid filled which reduced the mass transfer coefficient. In order to better condition the culture media, the solvent flow was controlled by pH feedback. This scenario showed comparable biomass productivity (0.10 g L^{-1} d^{-1}) to the conventional direct bubbling method, but with a lower energy cost and higher CO_2 utilization efficiency. Further, a pond liner was formed from flat sheet membranes as a more effective alternative to a hollow fiber arrangement. The optimized system achieved a CO_2 utilization efficiency of up to 90% compared to 47% with the uncontrolled hollow fiber membrane system and 11% for air sparging, thereby reducing the CO_2 released to the atmosphere.

Keywords

Carbon dioxide

Membrane

Nannochloropsis sp.

Potassium glycinate

Flow control

Abbreviations

PG	potassium glycinate
PDMS	polydimethylsiloxane
HFM	hollow fiber membrane
FSL	flat sheet liner
OD	optical density
DW	dry weight of biomass
MF	modified-F medium

1 Introduction

Annual anthropogenic CO_2 emissions have exceeded 3×10^{10} t since 2010 [1], driving research into technologies for CO_2 capture, utilization and storage. Besides geological sequestration and industrial utilization, CO_2 can be fed to photoautotrophic organisms. As an ideal biological CO_2 sink, microalgae show 10 to 50 times faster growth rate [2, 3] and 6-16 times higher photosynthetic efficiency [4] compared with terrestrial plants. Moreover, given its potential to produce biofuel, protein and high-valued nutraceuticals, microalgal fixation of CO_2 demonstrates its superiority both in environmental benignancy and economic feasibility [5].

Provision of inorganic carbon has long been acknowledged as crucial in microalgae cultivation, and the conventional method is sparging gas containing CO_2 (e.g., CO_2 enriched air, flue gas or purified CO_2) into the microalgae cultivation system. The major problem of sparging is that around 50%~90% [6] of the CO_2 escapes to the atmosphere without being effectively fixed, raising the cost of raw materials and in contradiction to the low carbon concept. Guria and coworkers[7] reduced the escape of CO_2 by bubbling a simulated flue gas through a controlled amount of NaOH, creating soluble carbonates and bicarbonates before contact with the algae culture. Alternatively, sodium bicarbonate can be directly added to enhance growth and lipid accumulation of microalgae [8]. However, these methods suffer due to the increased ionic strength and the inapplicability to microalgae species unable to take up bicarbonate [9].

The use of membranes in CO_2 supply has a shorter history. Basically, two methods of carbon supply by membranes have been suggested: membrane sparging and membrane contacting. The former creates small gas bubbles by sparging pressurized gas through microporous membranes. The smaller bubble size (1~2 mm) compared with that of conventional sparging (5~8 mm) accelerates mass transfer and thus reduces gas loss [10]. Membrane sparging can be

used as the main way of gas delivery or act as a CO_2 supplement to conventional sparging [10]. In contrast, membrane contacting transfers molecular CO_2 through a non-porous membrane layer which ensures that only individual molecules of CO_2 are able to transfer to the liquid side, without bubble formation. For example, Kim et al.[11] passed pure CO_2 through the inside of hollow fibre membranes that sandwiched a non-porous polyurethane layer between two porous polyethylene layers, to achieve bubbleless transfer.
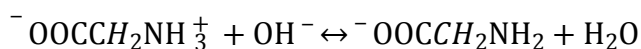
Liquid-liquid phase transfer of CO_2 to algal cultures was first applied by Pörs et al. [13] using a sealed low-density polyethylene bag containing $KHCO_3$-K_2CO_3 buffer solution. CO_2 molecules were released by the buffer solution and transferred across the polyethylene to promote the growth of cyanobacteria in a 50 mL flask. In our own work, we have transferred molecular CO_2 from a solvent such as potassium carbonate or potassium glycinate to a microalgae broth by using microporous hollow fibre membranes which are coated with a non-porous polydimethylsiloxane layer [15, 16].

There has been very limited research on liquid-liquid membrane contactors for delivering CO_2 and more investigations are needed to better understand its mechanisms and influencing factors. To date, the flowrate of CO_2 delivered to the algae culture has not been controlled, which has led to significant changes in the culture pH, thus influencing the growth of algae cells. Common methods of controlling pH in microalgae systems are acid/base titration [17-19] and CO_2 aeration [8, 17, 20]. Other methods include the use of proton and nutrient balanced medium [21] and the use of buffer systems combining bicarbonate and phosphate [22]. Among these, CO_2 aeration is considered more economic and benign as it avoids the use of chemicals and contributes to greenhouse gas utilization [20], although the problem of ventilation loss exists.

In this research, mass transfer experiments have been conducted with two different self-made membrane modules to shed light on the important parameters in liquid-liquid membrane contactor design. Importantly, the approach is then scaled up to be operated with an immersed flat sheet membrane liner contactor within a benchtop microalgae raceway pond. This system was designed to control the culture pH as well as the solvent flow without additional CO_2 dosing. The in-situ membrane contactor-pH control device is easy to maintain and to further upscale. Meanwhile, CO_2 loss to the atmosphere is minimized.

2   Materials and methods

2.1   CO$_2$ loaded solvent

20 wt% potassium glycinate (PG) solutions were prepared as the CO$_2$ solvent by mixing equimolar amounts of potassium hydroxide (Science supply, AR) and glycine (Chem-supply, AR) in ultrapure water (Millipore Elix), following the reaction in Eqn. 1. After cooling to room temperature, the solution was loaded by bubbling CO$_2$ (Eqn. 2). The CO$_2$ content was measured by a CM5015 CO$_2$ Coulometer (UIC Inc.) based on an acid titration mechanism. A specific CO$_2$ loading was then achieved by mixing PG solutions with known loadings at the necessary ratio.

$$^-OOCCH_2NH_3^+ + OH^- \leftrightarrow\ ^-OOCCH_2NH_2 + H_2O$$

<div align="right">Eqn. 1</div>

$$2\ ^-OOCCH_2NH_2 + CO_2 \leftrightarrow\ ^-OOCCH_2NH_3^+ +\ ^-OOCCH_2NHCOO^-$$

<div align="right">Eqn. 2</div>

2.2   Microalgae inoculum

A marine strain of *Nannochloropsis* sp. studied previously [23] was chosen as the model microalgae in our experiments due to its high biomass productivity, high lipid content, tolerance to varying conditions and the knowledge of its genome [24, 25]. A modified-F (MF) medium was prepared for algae growth [26]. As this research focused on the influence of CO$_2$ delivery, carbon sources were excluded from the medium. The microalgae stock was inoculated with MF medium to an optical density (OD) of 0.2 at 750 nm at the start of the experiments.

2.3   Membrane modules

Details of the membrane modules are listed in Table 1. The hollow fiber membrane (HFM, Airrane) used in the experiments consists of a microporous polysulfone support layer and a thin non-porous PDMS coating. Forty HFMs were glued together at both ends with a super-strength epoxy adhesive (Araldite, Selleys) to make a bundle that could be connected to tubing. Different fiber lengths (20, 30, 40, 50 cm) were prepared for the assessment of mass transfer performance. The flat sheet liner (FSL) was prepared by folding a flat sheet of PDMS-polysulfone membrane (PERVAP, DeltaMem AG) lengthways. An inert polymer spacer (Applied Membranes Inc.) with mesh size 8 and thickness 0.75 mm was placed between the two membrane sheets to form a flow channel. The two long edges of the membrane were glued

<div align="right">4</div>

together around the plastic mesh and then the two open short ends were glued around two 3D-printed distributors, thus forming an envelope for the solvent to flow inside (see Figure 1).

Module type	support layer [a]	selective layer [b]	Dimension (cm) [c]
HFM	polysulfone, 80 ± 7 μm	PDMS, 0.5 μm	L 20 × D 0.04 × 40
			L 30 × D 0.04 × 40
			L 40 × D 0.04 × 40
			L 50 × D 0.04 × 40
FSL	polysulfone, 48 ± 3 μm	PDMS, 5 μm	L 27 × W 5

Table 1 - Membrane module parameters

Note: a. acquired by an OLYMPUS BX51 microscope and consistent with the suppliers' information

b. based on the suppliers' information

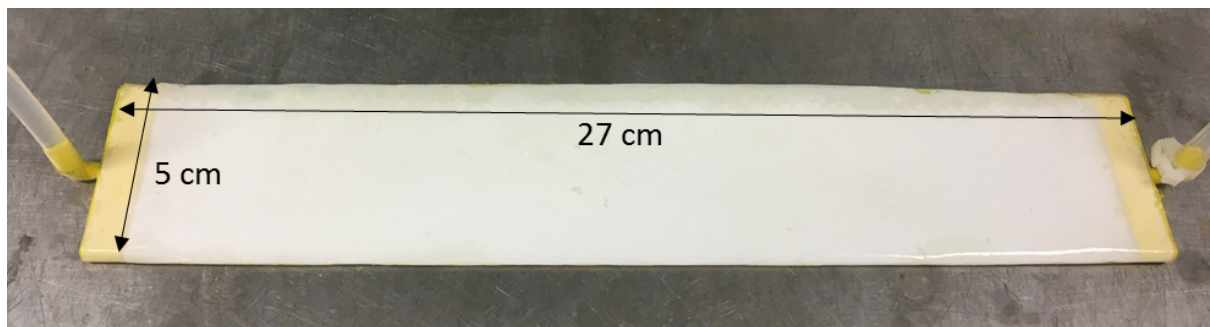c. L-length, D-outer diameter, W- width

Figure 1 - the flat sheet liner, formed by folding a flat sheet membrane lengthways, gluing together the open edges and then gluing the ends around 3D-printed distributors.

2.4 Raceway pond

A detailed structure of the benchtop raceway pond is shown in Figure 2. The tank has four identical channels (each with a capacity of 2.8 liters), allowing for different experimental conditions to be tested. Each channel has a baffle and a five-blade paddle wheel driven by a motor and rotated at 23 rpm to circulate the flow. The depth of the culture is 10 cm. Light is provided by four light tubes (Aqua T5 Aquarium Light 4×39W) hung above the lid, providing a continuous illumination of (120 ± 2) μmol m^{-2} s^{-1} at the culture surface. The culture temperature was 24 ± 2 °C with a difference no more than 1.0 °C between the four channels. Membranes could be submerged in the pond, isolating solvent and the microalgae while enabling CO_2 mass transfer. As a comparison, in some cases the microalgae were provided with the same light source and nutrients without air or CO_2 addition. In other cases, an air stone was placed at the bottom of the pond, diffusing air at a flow rate of 1.1 L$_{air}$ L$_{culture}$$^{-1}$ min^{-1} (1.1
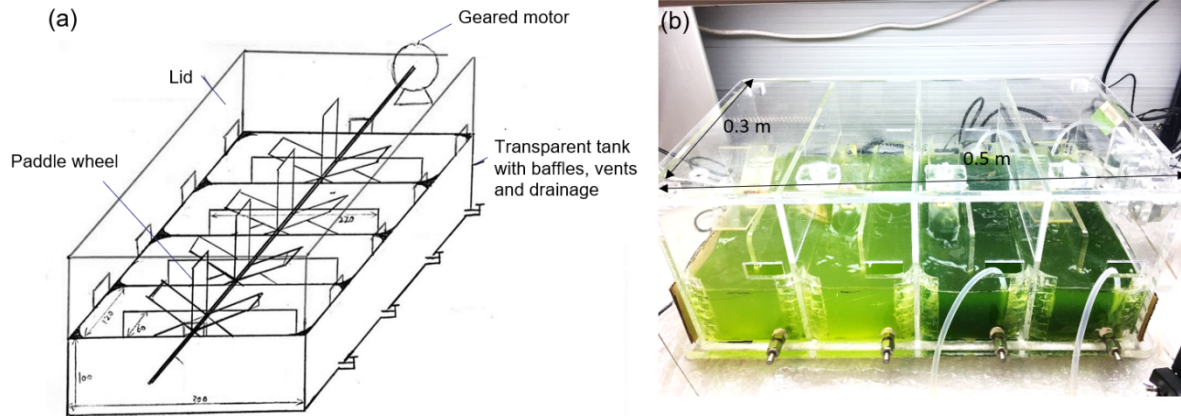
vvm).

Figure 2 - (a) A sketch of the benchtop raceway pond and (b) a photo of the benchtop raceway pond in operation with the microalgae in the right two channels being provided with CO_2 using a flat sheet liner while in the left two channels without.

2.5 CO_2 mass transfer experiments

To determine the actual CO_2 mass transfer rate, experiments were conducted in the solvent – membrane - MF medium system without microalgae. HFMs with different fiber lengths were tested in 400 mL continuously stirred MF medium in flasks, as described in our previous work [15]. Conversely, the upscaled FSLs with different loadings of solvents were tested in the raceway pond directly. During CO_2 mass transfer from the rich solvent to the lean medium, the pH in the medium was recorded. Within the pH range of these experiments, the CO_2 will react to form bicarbonate, so changes in the H^+ concentration, determined through changes in the pH, are linearly correlated with changes in the CO_2 concentration due to mass transfer across the membrane. The instant mass transfer rate can then be described by Eqn. 3 [12], where V is the liquid volume on the medium side (m^3), t is time (s), C is the H^+ concentration on the medium side (mol L^{-1}), K_L is the liquid phase overall mass transfer coefficient (m s^{-1}), A is membrane interface area (m^2) and C^* is the equilibrium H^+ concentration on the medium side (mol L^{-1}). C^* is a constant, thus Eqn. 3 can be integrated to Eqn. 4, where C_0 is the initial H^+ concentration on the medium side (mol L^{-1}). Therefore, a plot of the logarithmic concentration $\ln\frac{C^* - C_0}{C^* - C}$ versus time should be linear, with the mass transfer coefficient determined from the gradient. The experimental data fitted this model well.

$$VdC/dt = K_L A(C^* - C)$$

Eqn. 3

6

$$\ln\frac{C^* - C_0}{C^* - C} = \frac{A}{V}K_L t$$

<div align="right">Eqn. 4</div>

The gas phase overall mass transfer coefficient K_G (mol m^{-2} s^{-1} Pa^{-1}) can be calculated from K_L (Eqn. 5), where H is the Henry solubility of CO_2 at 24 °C (3.56×10^{-4} mol m^{-3} Pa^{-1} [27]). Membrane permeance could be estimated from K_G by the unit conversion Eqn. 6.

$$K_G = HK_L$$

<div align="right">Eqn. 5</div>

$$1GPU = 10^{-6}\frac{cm_{STP}^3}{cm^2 s \cdot cmHg} \rightarrow 3.33 \times 10^{-10} mol\, m^{-2} s^{-1} Pa^{-1}$$

<div align="right">Eqn. 6</div>

Also, the permeability of the support layer $P_{support}$ (Barrer) can be determined according to Eqn. 7, where R, R_{PDMS} and $R_{support}$ are the resistance of the whole membrane, the PDMS layer and the support layer respectively; l_{PDMS} and $l_{support}$ are the thickness of the two layers (μm). P_{PDMS} is assumed 1850 Barrer in our case [28].

$$R = \frac{1}{K_G} = R_{PDMS} + R_{support} = \frac{l_{PDMS}}{P_{PDMS}} + \frac{l_{support}}{P_{support}}$$

<div align="right">Eqn. 7</div>

2.6 Algae growing and controlling system

Figure 3 demonstrates the setup of the solvent – membrane – microalgae cultivation system with solvent flow control. CO_2 loaded solvent was pumped through semipermeable HFMs or the FSL in the microalgae raceway pond. CO_2 transfers across the membranes and is ultimately utilized by the algae cells to produce a lipid-rich biomass. In an industrial scenario, the lean solvent exiting from the algae pond would be transported back to the CO_2 absorber in a carbon capture plant for another absorption cycle. For simplicity, in this experiment, the solvent loading was kept at 0.50 ± 0.05 mol-CO_2/mol-PG by bubbling additional CO_2 daily into the solvent storage container.

An additional flow control system was applied to avoid the effects of dosing excessive CO_2. The pH meter (HI22091-02 Bechtop pH/mV Meter, Hanna Instruments) continuously detected the pH in the algae culture and output an analog signal through a Multifunction I/O Device (USB-6002, National Instruments) to a computer, where it was monitored using the software Labview 2018. The software then output a voltage signal to the peristaltic pump (Cole-Parmer

Masterflex L/S, John Morris Scientific) when the pH value was higher than 8.0, which is the optimal pH for the growth of *Nannochloropsis* sp. [29]. The pump started to operate when it received this non-zero signal, enabling CO_2 delivery via the solvent to decrease the culture pH.
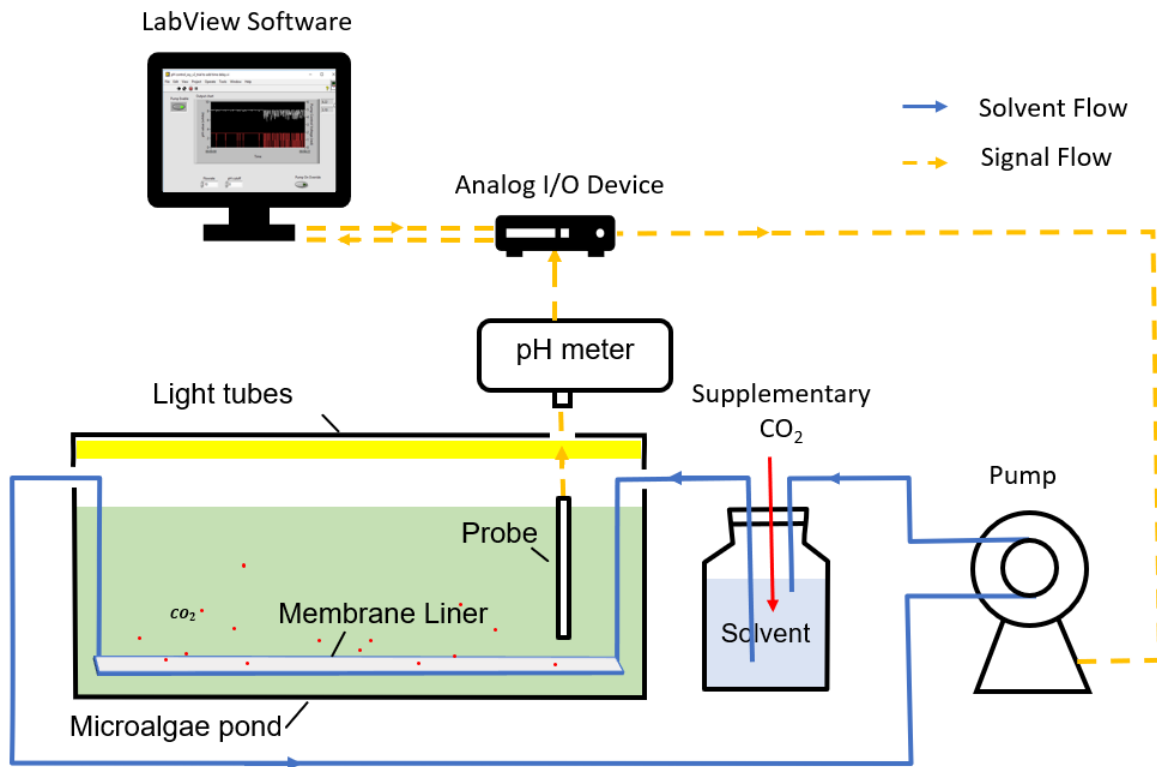

Figure 3 - The solvent-membrane-microalgae system with flow control.

2.7 Assessment of the microalgae growth

During microalgae cultivation, pH and temperature were in-situ measured by a pH meter (S220 SevenCompact™, Mettler Toledo). The OD of culture samples was measured by a UV-visible Spectrophotometer (Cary 300, Varian) at the wavelength 750 nm [30]. Based on multiple trials, there was a good linear correlation between the OD and dry weight (DW) of *Nannochloropsis* sp. when the OD was lower than 1.0 (DW (g/L) = 0.213 OD (R^2=0.982)). Therefore, during microalgae growth, culture samples were diluted to around 0.1 g/L and DW could then be conveniently estimated by Eqn. 8.

$$DW = 0.213 \times OD \text{ of diluted sample / dilution factor}$$

Eqn. 8

CO_2 concentration in the gas phase above the algae culture surface was measured by a Guardian Plus Infrared Gas Monitor (Edinburgh Sensors, UK). The amount of CO_2 transferred across the membrane (T_{CO_2}, mol) under continuous dosing mode could be determined according to

Eqn. 9, where Δp_{CO_2} is the partial pressure difference between the solvent and culture medium (Pa), which was determined in our previous study [31].

$$T_{CO_2} = K_G A t \Delta p_{CO_2}$$

<div align="right">Eqn. 9</div>

When solvent flow control was implemented to maintain constant pH, the solvent flow was intermittent while mass transfer was not. Therefore, it was difficult to calculate T_{CO_2} by Eqn. 9, as when the solvent flow was halted, the partial pressure associated with the solvent in the tubing gradually fell. To deal with this, another bottle of solvent was placed beside the feed container, with the same tubing and pump connections except the membranes and algae culture. T_{CO_2} was determined by the average daily difference in CO_2 loading between the experimental solvent and this control, immediately before this loading was restored to 0.5 through bubbling of additional CO_2.

The amount of CO_2 fixed by the microalgae F_{CO_2} (mol) was calculated according to Eqn. 10, where C_C is the carbon content of microalgae cells. Generally, $C_C \approx 0.5$ [32] and this value is used here. M_{CO_2} and M_C are the molar mass of CO_2 and carbon respectively (g mol^{-1}). P_b is the biomass productivity (g L^{-1} d^{-1}), which can be calculated by Eqn. 11. X_0 and X are the biomass concentration at the start and end of the cultivation period (g L^{-1}).

$$F_{CO_2} = P_b C_C (M_{CO_2}/M_C)$$

<div align="right">Eqn. 10</div>

$$P_b = (X - X_0)/t$$

<div align="right">Eqn. 11</div>

The CO_2 bio-utilization efficiency in a submerged membrane contactor was defined by Eqn. 12.

$$E = F_{CO_2}/T_{CO_2} \times 100\%$$

<div align="right">Eqn. 12</div>

3   Results and Discussion

3.1   Influence of membrane resistance on CO_2 mass transfer

Initial experiments were conducted without algae to determine the mass transfer coefficient from the change in medium pH. The membrane area of the FSL was lower than the HFM,

causing a relatively slower CO_2 transfer rate, which was indicated by the slower change in pH (see Supplementary Information). As detailed in Section 2.5, the overall mass transfer coefficient K_L acquired from the concentration data can be converted to a membrane permeance, which is theoretically constant for the same membrane materials. As confirmed in Table 2, K_L did not vary significantly with membrane area or solvent loading, with estimated values of (8.5 ± 1.1) ×10^{-6} m s^{-1} for HFM and (12.4 ± 2.2) ×10^{-6} m s^{-1} for FSL. These values are of the same order of magnitude to similar studies [12, 33]. Given the resistance per unit thickness of PDMS is known (1850 Barrer)$^{-1}$, that for the porous polysulfone layer can be estimated from Eqn. 7 as (680 ± 40 Barrer)$^{-1}$. It is clear from this analysis that the porous polysulfone provides most of the resistance to mass transfer, as it is considerably thicker in both cases than the PDMS layer and it has a lower permeance (Table 2). The thickness of the polysulfone layer in the HFM is greater than that of the FSL, which is the reason that the FSL has slightly higher membrane permeance (13.3 GPU) than the HFM (9.1 GPU).

Unlike gas separation or gas-liquid contacting, in these experiments there is a liquid phase on both sides of the membranes, thus it is expected that the microporous support is fully wetted. To confirm if this was the case, the permeability of a fully wetted polysulfone layer (based on the gas phase) was estimated from the formula:

$$P_{support} = \frac{l_{support}}{R_{support}} = \frac{\varepsilon \mathcal{D} H}{\tau}$$

Eqn. 13

Where $\mathcal{D}$ is the diffusivity of CO_2 in the liquid phase (assumed to be similar to that for CO_2 in water, so 1.77×10^{-9} m^2 s^{-1} at 25 ºC) and ε and τ are the porosity and tortuosity of the support layer. The tortuosity can, in turn, be estimated from [34, 35]:

$$\tau = \frac{(2 - \varepsilon)^2}{\varepsilon}$$

Eqn. 14

Using Eqn. 13 and Eqn. 14, a permeability of 680 Barrer will correspond to a porosity of 0.75 and a tortuosity of 2.1, which are realistic values for this type of support [36] and confirm that the support is substantially wetted. Given the high resistance of the support layer, the mass transfer in the membrane contactor could be improved by making the support layer thinner or excluding it altogether. One option might be to imbed a mechanical support within a pure PDMS layer, as is often done with ion exchange membranes. However, it is important to strike a balance between membrane cost and CO_2 flux.

To ensure a valid comparison, the HFM and FSL were used at a packing density of 12.6 and 10.5 $m^2_{membrane}/m^3_{culture}$ respectively during microalgae cultivation, so that their CO_2 flowrates were equivalent. These values are similar to the membrane areas used in a comparable membrane photobioreactor in the literature [37, 38].

Module Type	A/V (m^2/m^3)	Solvent loading	K_L (m s^{-1})	Average K_L (m s^{-1})	Membrane Permeance (GPU)	$R_{support}$ /R_{PDMS}
HFM	28.3	0.5	9.8×10^{-6}			
HFM	42.4	0.5	7.6×10^{-6}	(8.5 ± 1.1)	9.1	404
HFM	56.5	0.5	9.5×10^{-6}	$\times 10^{-6}$		
HFM	70.7	0.5	7.2×10^{-6}			
FSL	10.5	0.5	1.0×10^{-5}	(12.4 ± 2.2)	13.3	27
FSL	10.5	0.6	1.5×10^{-5}	$\times 10^{-6}$		

Table 2 - CO_2 mass transfer performance with various membrane modules, membrane areas and solvent loadings.

3.2 Membrane contacting with flow control

The medium pH influences enzyme activity in the cells and also affects the concentration of bicarbonate in the medium, thus indirectly influencing carbon assimilation by the microalgae [25]. In our prior work, the pH has not been controlled and this has led to poor algal growth in some cases [39]. In the present case, with no CO_2 addition at all, the pH in the control culture surged from 8.4 to 10.2 within three days (Figure 4(a)) as the carbon demand from the algae exceeded the supply from atmosphere. Due to the lack of a carbon source, the control culture had the lowest productivity (0.03 g L^{-1} d^{-1} or 3.2 g m^{-2} d^{-1}) as shown in Figure 4(b). Additionally, the dominant carbon species in the control culture converted from bicarbonate to carbonate, which cannot be utilized by most microalgae species [40]. When air was bubbled into the culture, CO_2 in the air dissolved in the medium, which significantly enhanced the productivity of the *Nannochloropsis* sp. culture (0.076 g L^{-1} d^{-1}). In the following discussion, this sparged culture is used as a positive control in terms of biomass growth. It should be mentioned that at large scale, CO_2 enriched air with 5~20 vol.% of CO_2 is more practical to use to enhance algae growth than pure air due to the large volumes required [41-43]. However, in this lab-scale research, the low concentration of CO_2 in air was compensated for by applying a sufficiently high air flow rate to avoid carbon limitation.

With HFMs continuously delivering CO_2 from the solvent to the culture, the pH in the medium was lower than that in the other trials (Figure 4(a)) due to the CO_2 supply exceeding the demand;

consistent with our earlier work [15, 31]. In particular, on the first day when the biomass concentration was low, the excessive CO_2 transferred to the algae medium led to an acidic environment. The effect of the low pH was compensated for by the availability of an ample carbon source, as the HFM group showed algae productivity of 0.089 g L^{-1} d^{-1}, comparable to the air sparging group (Figure 4(b)). While this indicates the tolerance of *Nannochloropsis* sp. to lower pH, the energy and material costs associated with pumping the solvent mean that it is necessary to avoid dosing CO_2 beyond demand. The HFM system with flow control achieved a biomass productivity of 0.10 g L^{-1} d^{-1} or 10.2 g m^{-2} d^{-1}. Within experimental error, this productivity is comparable, if not better than, that without flow control or with air sparging. Further, stopping the solvent flow whenever the pH fell below 8.0 reduced the pump working time to just 3% of cultivation time, which means the energy duty of the solvent pump was significantly reduced and the CO_2 in the solvent had a longer time to be effectively utilized. By contrast, the solvent in the uncontrolled HFM system needed to be reloaded with CO_2 more frequently, which resulted in its pH fluctuation (Figure 4(a)).

In addition to successfully preventing carbon limitation of the microalgae cultures, the membrane systems have significant advantages over direct bubbling. Firstly, due to the spontaneous solvent regeneration within the algae pond, the CO_2 chemical absorption strategy is more economically competitive [15]. Secondly, there is no need for gas compression and transportation. Instead, liquid solvent can be piped more economically across long distances, thus eliminating the necessity of locating a microalgal pond close to a CO_2 source. This benefit was significantly enhanced with the pH-controlled system, which greatly reduced the pumped volume required. Thirdly, gas loss to the atmosphere is minimized since CO_2 transfers as individual molecules rather than in gas bubbles. Finally, contamination from the CO_2 source (e.g. toxic inhibitors in the flue gas) is avoided since the solvent is isolated from the culture media by the membrane.
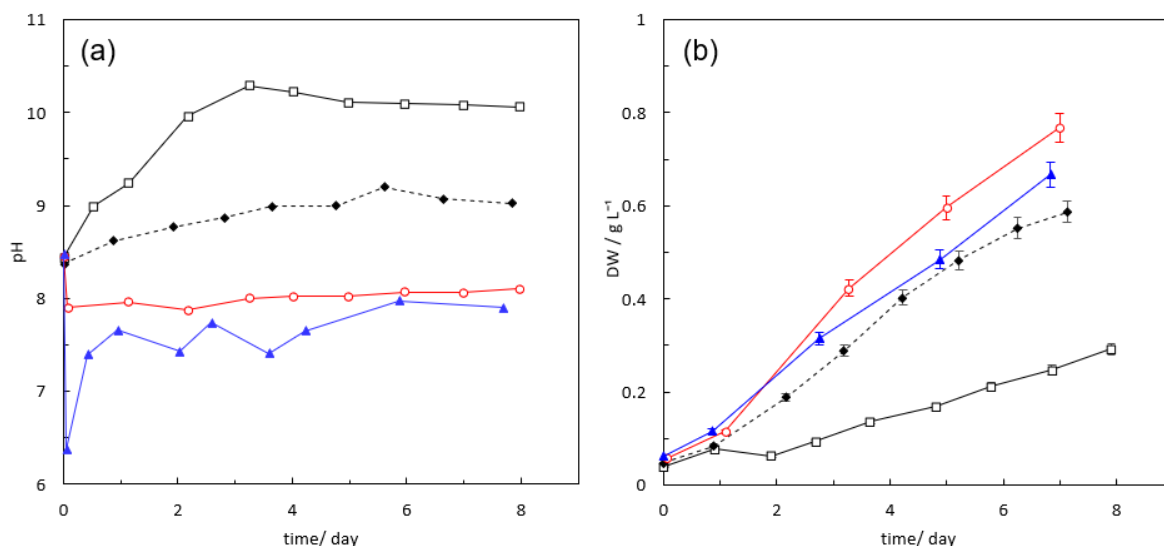
Figure 4 - (a) pH and (b) growth curves of *Nannochloropsis* sp. with no CO_2 addition (□); with air sparging as a source of CO_2 (♦); when solvent was supplied to a hollow fibre bundle of 0.03 m² with no pH control (▲); and when the solvent was supplied to the same hollow fibre bundle with pH control (○). Error bars are presented as 4.1% based on duplicate results.

3.3   Flat sheet liner

The FSL was investigated as an alternative to the HFMs in the membrane contacting application. The two membrane configurations achieved similar productivities (0.09 g L^{-1} d^{-1}) in the *Nannochloropsis* sp. cultures. Again, the flow control strategy could be applied to the FSL and appeared to achieve a higher growth (Figure 5(b)). Unlike in the HFM system, the pH in the FSL system was higher than 8 (Figure 5(a)). This was because the FSL had a larger volume capacity than the HFMs, thus the solvent retention time was longer and the pH fell more slowly. Another reason was that, although the surface below the FSL was capable of mass transfer, there was no algae in this region and so this CO_2 needed to migrate to the top surface. This lower CO_2 flux could be readily avoided by using a greater membrane area, or by reducing the resistance of the membrane support layer as discussed above. Potential advantages of the FSL over the HFM are that it is more convenient for maintenance and cleaning and should be less susceptible to physical damage than the hollow fibers. Also, the FSL can be laid at the bottom of the raceway pond, avoiding light shading to the bulk culture caused by the floating hollow fiber membranes.
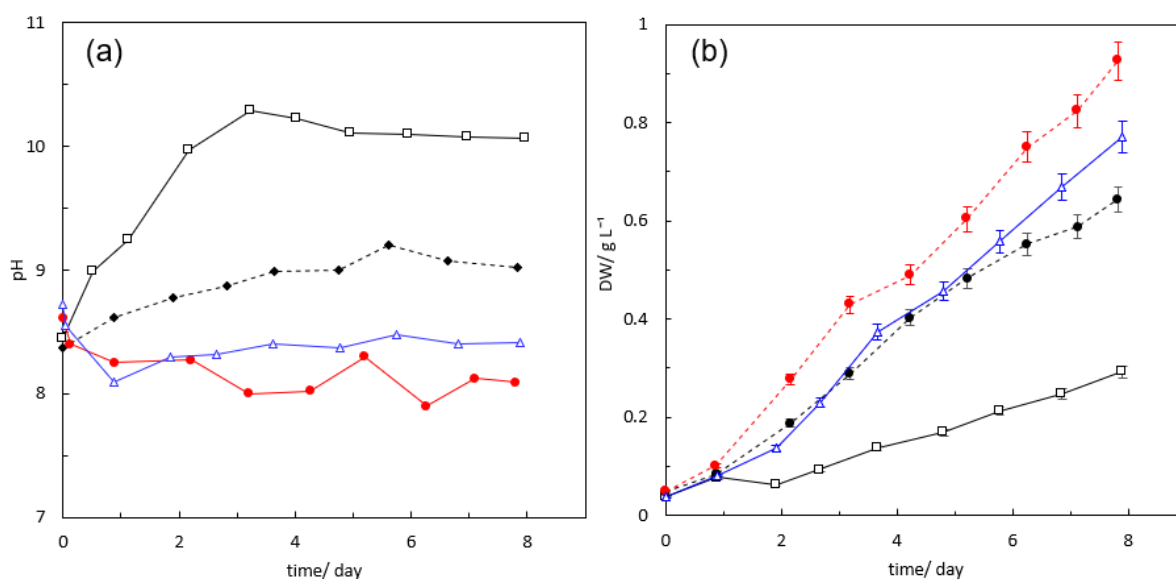
Figure 5 - (a) pH and (b) growth curves of *Nannochloropsis* sp. with no CO_2 addition (□); with air sparging as a source of CO_2 (♦); when solvent was supplied to a FSL of 0.03 m^2 with no pH control (Δ); and when the solvent was supplied to the same FSL with pH control (●). Error bars are presented at 4.1% according to specific duplicates.

Figure 6 indicates the amount of CO_2 that escapes to the gas phase under different cultivation conditions. There was no significant change during the cultivation period, indicating a stable CO_2 release-utilization-ventilation chain. Photosynthesis utilizes CO_2 to produce biomass, and hence the CO_2 content above the control group was only half of that in the atmosphere. This again indicated that the growth of the microalgae was limited by the carbon source. When HFMs were introduced to continuously deliver CO_2 to the algae culture, the CO_2 content in the gas phase rose dramatically to 1600 ± 50 ppm, indicating that some of the CO_2 escaped without being biologically fixed because of the excessive dosing of CO_2 and the insufficient distance between the floating membrane fibers and the culture surface. However, the flow control mode discussed in Section 3.2 decreased the CO_2 concentration in the headspace by 69%, reducing CO_2 loss by preventing unnecessary CO_2 from being delivered. The FSL showed similar CO_2 gas phase concentrations even without pH control, due to the greater distance between the liner and the surface of the media. When the solvent flow was controlled inside the FSL, the CO_2 concentration in the headspace further decreased to 380 ± 50 ppm, which was 76% lower than for the uncontrolled HFM regime; and within experimental error the same as in the atmosphere a distance from the experimental setup. This confirms that the pH control system was able to match the CO_2 supply to the demand.
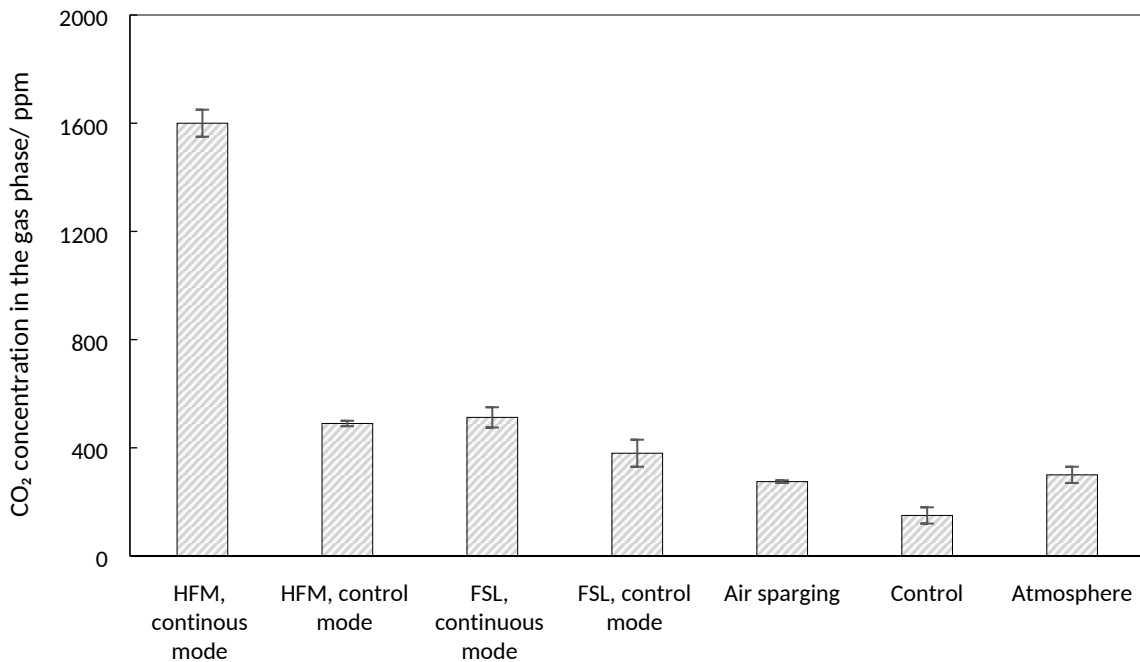
Figure 6 - CO_2 content in the gas phase above the algae cultures. Error bars represented the ranges of triplicate measurements on individual days.

Error! Reference source not found. Table 3 compares the CO_2 utilization efficiency for three of the tested CO_2 delivery systems and for conventional CO_2 dosing systems reported in the literature. With air sparging at a flowrate of 1.1 vvm, only 11% of CO_2 was fixed by the algae cells. The bubbles diffusing from the air stone had a diameter of around 5 mm. This suggests a velocity of 0.25 m s^{-1} and hence a residence time in the pond of only 0.4 second. While the mass transfer coefficient from these free bubbles is estimated as being 20 times higher than through the flat sheet liner (2.7×10^{-4} m s^{-1} using Christi et al.[44]), this short residence time and the low CO_2 concentration inside the bubbles results in poor utilization.

When the PDMS membrane was used, the mechanism of CO_2 transfer is solution diffusion. In this case, only individual CO_2 molecules entered the media, confirmed by an absence of visible gas bubbles. In this case, it took a longer time for the CO_2 to leave the liquid phase. The CO_2 fixation efficiency of the HFM without pH control rose four times higher than that when gas bubbles existed (Table 3). It should be mentioned that this result does not contradict with the high CO_2 concentration in Figure 6, as the CO_2 that escaped in the air sparging scenario was "diluted" with the other 99.97% gas species in the air, while membranes delivered pure CO_2 that accumulated in the gas phase. As a further improvement, the combined FSL and flow control system captured 90% of the CO_2 that transferred across the membranes. This efficiency is higher than that of conventional CO_2 sparging systems with pH control (about 75%) [45, 46].

15

It was estimated that CO_2 takes up 71% of the raw material costs (1.09 USD/kg biomass) in a pilot scale microalgae production plant with production capacity of 3.8t/year [45]. On this basis, an improvement of CO_2 utilization efficiency by 15% will contribute to a reduction by 0.12 USD/kg biomass produced. However, this is a conservative estimate, as it does not account for the penalties that may apply for the release of this CO_2 into the atmosphere into the future.

Table 3 - CO_2 utilization efficiency for different systems.

Carbon source	Availability of pH control	CO_2 utilization Efficiency
Air sparging	No	(10.7 ± 0.4) %
CO_2 through HFM	No	(47 ± 2) %
CO_2 sparging	Yes	74.5% [45]
CO_2 enriched air sparging	Yes	75.6% [46]
CO_2 through FSL	Yes	(90 ± 4) %

4 Conclusions

A CO_2 solvent-membrane-microalgae contactor has been investigated which enables biological utilization of CO_2 as a low energy means for solvent regeneration, while also enhancing microalgae productivity. The CO_2 mass transfer coefficient for the HFM and FSL were 8.5×10^{-6} m s^{-1} and 1.2×10^{-5} m s^{-1} respectively. As the support material contributed most of the membrane resistance, a recommended improvement is to reduce or eliminate this support layer without compromising the mechanical strength. Controlling the solvent flow to maintain the culture pH at 8.0 avoided excessive dosing of CO_2 to the microalgae culture and avoided the energy needed for continuous pump operation. In this case, a biomass productivity of 0.10 g L^{-1} d^{-1} comparable to the conventional aeration method was achieved. The FSL provides a better membrane configuration compared with the HFM, because of the convenience of cleaning and maintenance, the lack of light shading and also the potential to reduce the CO_2 loss. With the flow controlled inside the FSL, the CO_2 bio-utilization efficiency increased up to 90%.

5 Acknowledgements

6   References

[1] Global Energy and CO2 Status Report - 2017, in, International Energy Agency, 2018.

[2] M. Anjos, B.D. Fernandes, A.A. Vicente, J.A. Teixeira, G. Dragone, Optimization of CO2 bio-mitigation by Chlorella vulgaris, Bioresource Technology, 139 (2013) 149-154.

[3] M.J. Raeesossadati, H. Ahmadzadeh, M.P. McHenry, N.R. Moheimani, CO2 bioremediation by microalgae in photobioreactors: Impacts of biomass and CO2 concentrations, light, and temperature, Algal Research, 6 (2014) 78-85.

[4] P.J.l.B. Williams, L.M.L. Laurens, Microalgae as biodiesel & biomass feedstocks: Review & analysis of the biochemistry, energetics & economics, Energy & Environmental Science, 3 (2010) 554-590.

[5] A. Kumar, S. Ergas, X. Yuan, A. Sahu, Q. Zhang, J. Dewulf, F.X. Malcata, H. van Langenhove, Enhanced CO2 fixation and biofuel production via microalgae: recent developments and future directions, Trends in Biotechnology, 28 (2010) 371-380.

[6] J. Doucha, F. Straka, K. Lívanský, Utilization of flue gas for cultivation of microalgae Chlorella sp.) in an outdoor open thin-layer photobioreactor, Journal of Applied Phycology, 17 (2005) 403-412.

[7] A. Kumari, V. Sharma, A.K. Pathak, C. Guria, Cultivation of Spirulina platensis using NPK-10:26:26 complex fertilizer and simulated flue gas in sintered disk chromatographic glass bubble column, Journal of Environmental Chemical Engineering, 2 (2014) 1859-1869.

[8] E.J. Lohman, R.D. Gardner, T. Pedersen, B.M. Peyton, K.E. Cooksey, R. Gerlach, Optimized inorganic carbon regime for enhanced growth and lipid accumulation in Chlorella vulgaris Luisa Gouveia, Biotechnology for Biofuels, 8 (2015).

[9] Q. Zheng, X. Xu, G.J.O. Martin, S.E. Kentish, Critical review of strategies for CO2 delivery to large-scale microalgae cultures, Chinese Journal of Chemical Engineering, (2018).

[10] E. Suali, R. Sarbatly, S. Anisuzzaman, F. Abd Lahin, M.A. Asidin, T. Jusnukin, Effect of membrane on carbonation and carbon dioxide uptake of Chlorella sp, in: H.A. Abdulbari (Ed.), EDP Sciences, 2017.

[11] H.W. Kim, A.K. Marcus, J.H. Shin, B.E. Rittmann, Advanced Control for Photoautotrophic Growth and CO2-Utilization Efficiency Using a Membrane Carbonation Photobioreactor (MCPBR), Environmental Science & Technology, 45 (2011) 5032-5038.

[12] B.S. Ferreira, H.L. Fernandes, A. Reis, M. Mateus, Microporous hollow fibres for carbon dioxide absorption: Mass transfer model fitting and the supplying of carbon dioxide to microalgal cultures, Journal of Chemical Technology & Biotechnology, 71 (1998) 61-70.

[13] Y. Pörs, A. Wüstenberg, R. Ehwald, A batch culture method for microalgae and cyanobacteria with CO2 supply through polyethylene membranes, Journal of Phycology, 46 (2010) 825-830.

[14] J.D. Noel, W.J. Koros, B.A. McCool, R.R. Chance, Membrane-mediated delivery of carbon dioxide for consumption by photoautotrophs: Eliminating thermal regeneration in carbon capture, Industrial and Engineering Chemistry Research, 51 (2012) 4673-4681.

[15] Q. Zheng, G.J.O. Martin, S.E. Kentish, Energy efficient transfer of carbon dioxide from flue gases to microalgal systems, Energy & Environmental Science, 9 (2016) 1074-1082.

[16] Q. Zheng, G.J. Martin, Y. Wu, S.E. Kentish, The use of monoethanolamine and potassium glycinate solvents for CO2 delivery to microalgae through a polymeric membrane system, under review, Biochemical Engineering Journal, 128 (2017) 126-133.

[17] S. Huo, Z. Wang, S. Zhu, W. Zhou, R. Dong, Z. Yuan, Cultivation of Chlorella zofingiensis in bench-scale outdoor ponds by regulation of pH using dairy wastewater in winter, South China, Bioresource Technology, 121 (2012) 76-82.

[18] Q. Gong, Y. Feng, L. Kang, M. Luo, J. Yang, Effects of light and pH on cell density of Chlorella Vulgaris, Energy Procedia, 61 (2014) 2012-2015.

[19] N.R. Moheimani, Inorganic carbon and pH effect on growth and lipid productivity of Tetraselmis suecica and Chlorella sp (Chlorophyta) grown outdoors in bag photobioreactors, Journal of Applied Phycology, 25 (2013) 387-398.

[20] C.-Y. Chen, P.-C. Kao, C.H. Tan, P.L. Show, W.Y. Cheah, W.-L. Lee, T.C. Ling, J.-S. Chang, Using an innovative pH-stat CO2 feeding strategy to enhance cell growth and C-phycocyanin production from Spirulina platensis, Biochemical Engineering Journal, 112 (2016) 78-85.

[21] W. Tan, A.A. Adebusuyi, Proton and nutrient balanced medium for scalable, practical pH control in high-density Chlorella vulgaris cultures, Algal Research, 16 (2016) 119-126.

[22] Y.Y. Choi, J.M. Joun, J. Lee, M.E. Hong, H.-M. Pham, W.S. Chang, S.J. Sim, Development of large-scale and economic pH control system for outdoor cultivation of microalgae Haematococcus pluvialis using industrial flue gas, Bioresource Technology, 244 (2017) 1235-1244.

[23] R. Halim, D.R.A. Hill, E. Hanssen, P.A. Webley, S. Blackburn, A.R. Grossman, C. Posten, G.J.O. Martin, Towards sustainable microalgal biomass processing: anaerobic induction of autolytic cell-wall self-ingestion in lipid-rich Nannochloropsis slurries, Green Chemistry, (2019).

[24] J. Liu, Y. Song, W. Qiu, Oleaginous microalgae Nannochloropsis as a new model for biofuel production: Review & analysis, Renewable and Sustainable Energy Reviews, 72 (2017) 154-162.

[25] S.-Y. Chiu, C.-Y. Kao, M.-T. Tsai, S.-C. Ong, C.-H. Chen, C.-S. Lin, Lipid accumulation and CO2 utilization of Nannochloropsis oculata in response to CO2 aeration, Bioresource Technology, 100 (2009) 833-838.

[26] I.L.D. Olmstead, D.R.A. Hill, D.A. Dias, N.S. Jayasinghe, D.L. Callahan, S.E. Kentish, P.J. Scales, G.J.O. Martin, A quantitative analysis of microalgal lipids for optimization of biodiesel and omega-3 production, Biotechnology and Bioengineering, 110 (2013) 2096-2104.

[27] C.L. Yaws, Yaws' Handbook of Properties for Aqueous Systems, Knovel Norwich, NY, 2012.

[28] C.A. Scholes, G.W. Stevens, S.E. Kentish, The effect of hydrogen sulfide, carbon monoxide and water on the performance of a PDMS membrane in carbon dioxide/nitrogen separation, Journal of Membrane Science, 350 (2010) 189-199.

[29] J.M.S. Rocha, J.E.C. Garcia, M.H.F. Henriques, Growth aspects of the marine microalga Nannochloropsis gaditana, Biomolecular Engineering, 20 (2003) 237-242.

[30] M.J. Griffiths, C. Garcin, R.P. van Hille, S.T.L. Harrison, Interference by pigment in the estimation of microalgal biomass concentration by optical density, J. Microbiol. Methods, 85 (2011) 119-123.

[31] Q. Zheng, G.J.O. Martin, Y. Wu, S.E. Kentish, The use of monoethanolamine and potassium glycinate solvents for CO2 delivery to microalgae through a polymeric membrane system, Biochemical Engineering Journal, 128 (2017) 126-133.

[32] V. Mortezaeikia, O. Tavakoli, R. Yegani, M. Faramarzi, Cyanobacterial CO2 biofixation in batch and semi-continuous cultivation, using hydrophobic and hydrophilic hollow fiber membrane photobioreactors, Greenhouse Gases: Science and Technology, 6 (2016) 218-231.

[33] A. Kumar, X. Yuan, A.K. Sahu, J. Dewulf, S.J. Ergas, H. Van Langenhove, A hollow fiber membrane photo-bioreactor for CO_2 sequestration from combustion gas coupled with wastewater treatment: a process engineering approach, Journal of Chemical Technology & Biotechnology, 85 (2010) 387-394.

[34] S. Iversen, V. Bhatia, K. Dam-Johansen, G. Jonsson, Characterization of microporous membranes for use in membrane contactors, Journal of Membrane Science, 130 (1997) 205-217.

[35] J. Mackie, P. Meares, The diffusion of electrolytes in a cation-exchange resin membrane I. Theoretical, Proc. R. Soc. Lond. A, 232 (1955) 498-509.

[36] H. Yasuda, J. Tsai, Pore size of microporous polymer membranes, Journal of Applied Polymer Science, 18 (1974) 805-819.

[37] L.-H. Fan, Y.-T. Zhang, L.-H. Cheng, L. Zhang, D.-S. Tang, H.-L. Chen, Optimization of Carbon Dioxide Fixation by Chlorella vulgaris Cultivated in a Membrane-Photobioreactor, Chemical Engineering & Technology, 30 (2007) 1094-1099.

[38] L. Cheng, L. Zhang, H. Chen, C. Gao, Carbon dioxide removal from air by microalgae cultured in a membrane-photobioreactor, Separation and Purification Technology, 50 (2006) 324-329.

[39] Q. Zheng, G. Martin, S. Kentish, The effects of medium salinity on the delivery of carbon dioxide to microalgae from capture solvents using a polymeric membrane system, Journal of Applied Phycology, (2018) 1-8.

[40] A. Richmond, Handbook of microalgal culture: biotechnology and applied phycology, Wiley Online Library, 2004.

[41] J. Assunção, A.P. Batista, J. Manoel, T.L. da Silva, P. Marques, A. Reis, L. Gouveia, CO_2 utilization in the production of biomass and biocompounds by three different microalgae, Eng. Life Sci., 17 (2017) 1126-1135.

[42] S.F. Mohsenpour, N. Willoughby, Effect of CO_2 aeration on cultivation of microalgae in luminescent photobioreactors, Biomass and Bioenergy, 85 (2016) 168-177.

[43] S. Van Den Hende, H. Vervaeren, N. Boon, Flue gas compounds and microalgae: (Bio-)chemical interactions leading to biotechnological opportunities, Biotechnology Advances, 30 (2012) 1405-1424.

[44] Y. Chisti, Airlift Bioreactors, Elsevier Applied Science, Essex, UK, 1989.

[45] F.G. Acién, J.M. Fernández, J.J. Magán, E. Molina, Production cost of a real microalgae production plant and strategies to reduce it, Biotechnology Advances, 30 (2012) 1344-1353.

[46] Y. Jiang, W. Zhang, J. Wang, Y. Chen, S. Shen, T. Liu, Utilization of simulated flue gas for cultivation of Scenedesmus dimorphus, Bioresource Technology, 128 (2013) 359-364.

SUPPLEMENTARY INFORMATION

Enhanced CO_2 bio-utilization by an immersed membrane contactor in a bench-scale microalgae raceway pond

X. Xu [a,b], G. J. O. Martin [b], S. E. Kentish [a*]

[a] Peter Cook Centre for CCS Research, Department of Chemical Engineering, The University of Melbourne, Parkville, Victoria 3010, Australia.

[b] Algal Processing Group, Department of Chemical Engineering, The University of Melbourne, Parkville, Victoria 3010, Australia
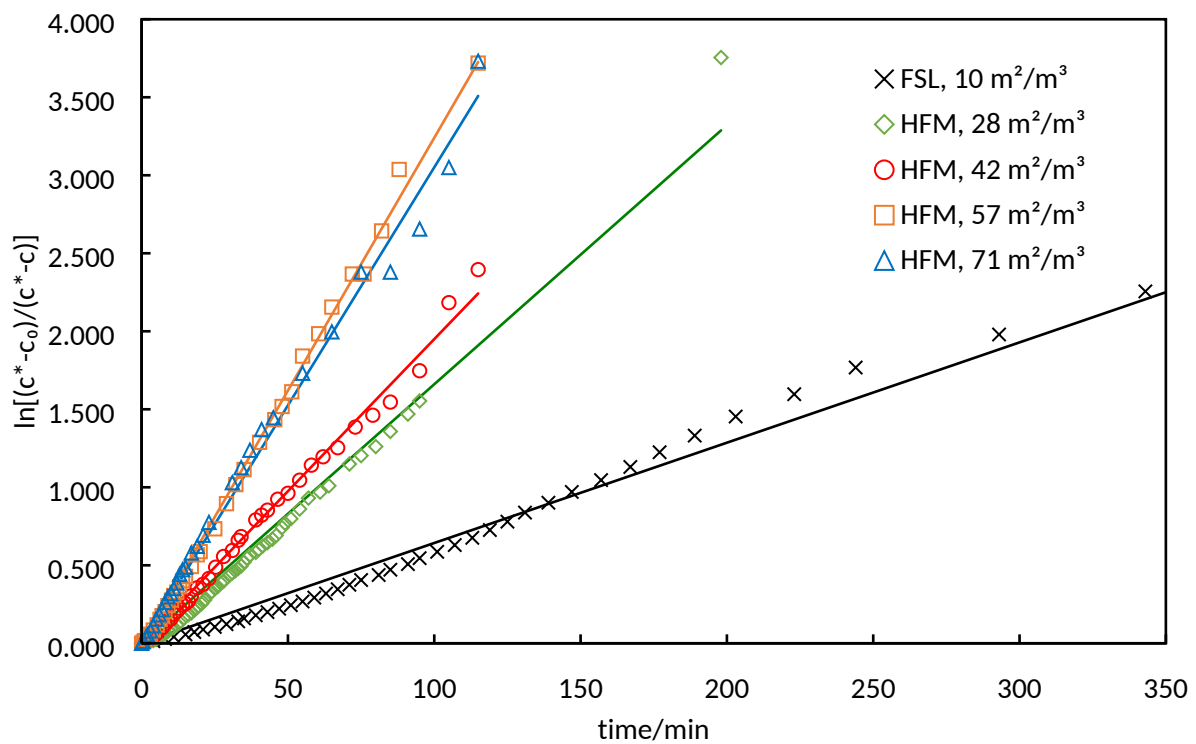
Figure S1 The linearized hydrogen ion concentration in the medium during CO_2 mass transfer from potassium glycinate (loading 0.5) across different types and lengths of membranes

Author/s:
Xu, X; Martin, GJO; Kentish, SE

Title:
Enhanced CO2 bio-utilization with a liquid-liquid membrane
contactor in a bench-scale microalgae raceway pond

Date:
2019-12-01

Citation:
Xu, X., Martin, G. J. O. & Kentish, S. E. (2019). Enhanced CO2 bio-utilization with a liquid-
liquid membrane
contactor in a bench-scale microalgae raceway pond. Journal of CO2 Utilization, 34, pp.207-
214. https://doi.org/10.1016/j.jcou.2019.06.008.

Persistent Link:
http://hdl.handle.net/11343/227156

File Description:
Submitted version